Pure Photoorientation of Azo Dye in Polyurethanes and Quantification of Orientation of Spectrally Overlapping Isomers

Zouheir Sekkat,*,†,‡ Daisuke Yasumatsu,† and Satoshi Kawata†

Department of Applied Physics and Handai Frontier Research Center, Osaka University, Suita, Osaka 565-0871, Japan, and School of Science and Engineering, Al Akhawayn University in Ifrane, 53000 Ifrane, Morocco

Received: January 16, 2002; In Final Form: July 8, 2002

We show that the occurrence of pure photoorientation by photoisomerization of azo dye in polymers is influenced by the polymer molecular structure, as well as by the photoisomerization quantum yields and the cis → trans thermal isomerization rate. These findings are rationalized by the study of the photoorientation of azo dye in a series of polyurethane polymers, each with distinct differences in the molecular structure of the unit building blocks. It will be shown that the thermally activated chromophore movement in these polymers is dictated by the polymer backbone. We also show how to quantify coupled photoisomerization and photoorientation of spectrally overlapping isomers in polymers, and we determine the photoisomerization quantum yields and the photoorientation movement of the chromophores in azo-polyurethanes.

I. Introduction

Phototriggered molecular movement by isomeric structural and orientational rearrangement of photoisomerizable chromophores in thin polymer films has been intensively researched with views of application in electrooptical modulation and optical data storage.[1−52] Light can manipulate the orientation of the chromophore by photoisomerization via polarized transitions, so the film's centrosymmetry and isotropy are alleviated, and anisotropy[11−13] and quadratic[6−10] and cubic[14] optical nonlinearities are induced far below the polymer's glass-transition temperature, T_g. Spontaneous molecular movement in polymers becomes increasingly appreciable as the operating temperature approaches T_g.[53] Inasmuch as sub-T_g optical ordering of photoisomerizable molecules is being intensively studied, its theoretical quantification is necessary to bridge independent studies in the areas of photochemistry and nonlinear optics.[18−22]

Recent studies on photoorientation processes in amorphous polymers have addressed the role of T_g and polymer structural effects, including the main chain rigidity, the nature of the connection of the chromophore to a rigid or semirigid or a flexible main chain, the free volume, the free volume distribution, or a combination of these.[49,50] The polymer structure and T_g are not the only important parameters for polymers, but the molecular weight and its distribution are also important. In fact, the glass relaxation is characterized by T_g, which is affected by several factors including the molecular weight, swelling, and cross-linking. In this paper, we discuss to what extent the polymer structure can influence chromophores photoorientation in a series of azo-polyurethane polymers, and we show that the occurrence of pure photoorientation depends on the structure of the polymer. We also develop the analytical theory of photoorientation of spectrally overlapping isomers, and we use it to quantify the photoorientation movement of azobenzene derivatives in films of azo-polyurethanes. The paper is organized as follows. In section 2, we discuss the structural features of the azo-polyurethanes studied and the photoorientation experimental methods, and in section 3, we discuss near-pure photoorientation observations and polymer structural effects experiments. In section 4, we quantify the photoorientation movement of the chromophores in the polymers studied. The analytical theory of photoorientation by photoisomerization in A ↔ B photoisomerizable systems where B is unknown is detailed in the Appendix, and in section 5, we conclude and give some remarks on the analysis.

II. Photoorientation Experimental Methods

Four azo-polyurethane derivatives used in our study, PUR-1, PUR-2, PUR-3, and PUR-4, each with distinct differences in the molecular structure of the unit building blocks, are shown in Figure 1. The T_g of PUR-1 and PUR-2 was 140 °C, while the T_g of PUR-3 and PUR-4 was 136 °C, as measured by differential scanning calorimetry. These azo-PUR polymers were commercial samples (Chromophore Inc.). All of these polymers are donor-embedded systems, in which the chromophore is incorporated flexibly into the backbone of the polymer through the electron-donating substituent. The azo chromophore in PUR-1 and -2 has a nitro, NO_2, electron-withdrawing group versus a cyano, CN, for PUR-3 and -4, a feature that slightly decreases the T_g and blue-shifts the maximum of absorption (see Figure 2 for the polymers spectra) and concomitantly slows the cis → trans thermal back isomerization of the azo dye in PUR-3 and -4. The difference between PUR-1 and -3 and PUR-2 and -4 is the aromatic ring in the polymer backbone, a seemingly small structural difference that does not affect the polymer T_g but that noticeably affects the orientation dynamics of the polymers. It will be shown that the photoorientation dynamics of azo-PURs are influenced not only by the polymer structure but also by the rate of the cis → trans thermal isomerization. Azo-PURs represent a good example of donor-embedded polymers in which both the ethylene spacers and the donor portion of the chromophore are incorporated into the polymer backbone. The particular structure of the azo-PUR systems

* To whom correspondence should be addressed.
† Osaka University.
‡ Al Akhawayn University in Ifrane.

10.1021/jp020132+ CCC: $22.00
Published on Web 11/12/2002

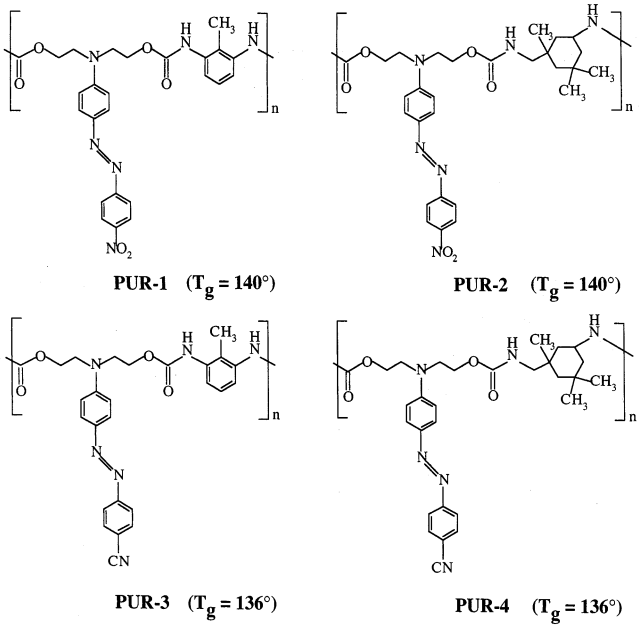

Figure 1. Chemical structures of the azo-PUR polymers.

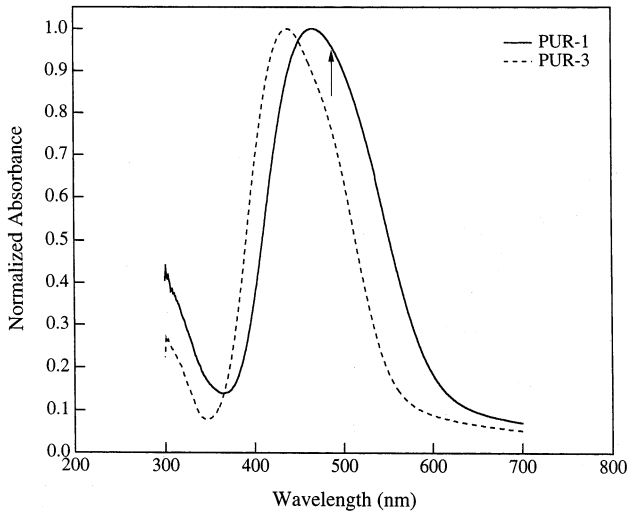

Figure 2. Normalized spectra of PUR-1 and -3. The spectra are normalized by the value of the maximum absorbance, and the arrow indicates the irradiation and analysis wavelength.

studied enables a very high chromophore concentration per weight relative to the polymer backbone (~80 wt % in azo-PURs vs, for example, 40% and 15% in azo-polyimides and azo-poly(methyl methacrylate) (azo-PMMA) copolymers, respectively), whereby the chromophore is tethered at both ends to the polymer main chain, a feature that enables an efficient coupling of the movements of the main chain and the chromophore and makes it easier for the backbone to respond to the photoinduced movement of the chromophores. Such structural features should improve the efficiency of photoorientation of the chromophores.

We have performed nonpolar photoorientation studies on the azo-PUR polymer series shown in Figure 1. For sample preparation, the polymer powders were used as received and were dissolved in cyclohexanone at a weight concentration of 10%, and filtered two times through 0.2 μm filters. Polymer films were spin-cast from solution onto glass substrates, heated above T_g to 150 °C for 1 h to remove residual solvent, and allowed to slowly cool to room temperature. The films thus prepared were about 80 nm thick and optically clear. We used real-time dichroism experiments to investigate the dynamics of photoorientation of the azo chromophores in films of PURs. Photoisomerization of the chromophores in the polymer was induced with linearly polarized blue pump light ($\lambda = 488$ nm) from an argon-ion laser. With consideration of the chromophore density (e.g., $\sim 20 \times 10^{20}$ molecules cm^{-3}) of the polymers, the irradiation intensity range imposes about 0.14 to 13.5 and 0.03 to 11.6 incident photons per chromophore per second for PUR-1 and -2 and PUR-3 and -4, respectively. In situ transmittance measurements were performed with a probe light polarized either parallel or perpendicular to the initial irradiating light polarization. The probe beam was propagating perpendicular to the plane of the sample and linearly polarized at 45° with respect to the plane of incidence of the irradiating beam. The transmitted parallel and perpendicular components were separated by a Wollaston prism and detected separately. The probe beam was also the blue light ($\lambda = 488$ nm, power ≈ 1 μW, and ~1 mm-diameter spot) of the argon-ion laser the output beam of which was split by a beam splitter to produce both the pump and probe beams. Dark conditions were employed to avoid the influence of the room light on the isomerization reaction.

$Abs_{||}$ and $Abs_{\perp}$ were calculated from the amount of absorbed light polarized parallel and perpendicular to the irradiation light polarization, respectively, and the isotropic absorbance, $\bar{A} = (Abs_{||} + 2Abs_{\perp})/3$, the anisotropy, $\Delta A = Abs_{||} - Abs_{\perp}$, and the spectral order parameter, $S = (Abs_{||} - Abs_{\perp})/(Abs_{||} + 2Abs_{\perp})$, were deduced. S was calculated at the steady state of photoorientation. Each photoorientation experiment has been done on a different previously nonirradiated sample so as to avoid irradiation history complications. The samples had similar absorbance values prior to irradiation, and the samples absorbances were accounted for in photoisomerization and photoorientation quantification (vide infra).

III. Polymer Structural Effects and Near-Pure Photoorientation

Figures 3, 4, and 5 show the time evolution of $Abs_{||}$ and $Abs_{\perp}$ of PUR-1, PUR-3, and PUR-2 before, during, and after linearly polarized irradiation for different irradiation power values, respectively. The real-time photoorientation of PUR-4 (not shown) shows a dynamical behavior similar to that of PUR-3, and all four PURs show the same dynamical behavior of ΔA; therefore, only that of PUR-1 is shown (Figure 3b). When irradiation starts at time $t = 5$ min, anisotropy occurs and demonstrates chromophore photoorientation, and when irradiation is turned off at time $t = 10$ min, the observed relaxation indicates that cis → trans thermal isomerization, which is completed after few seconds in PUR-1 and -2 and takes several minutes to more than an hour in PUR-3 and -4, converts cis to trans isomers, and the remnant anisotropy demonstrates that the trans molecules are oriented after isomerization. The CN electron-withdrawing group of the azo chromophore in PUR-3 and -4 slows the cis → trans thermal isomerization. Figure 6 shows that the isotropic absorbance of PUR-1 is recovered more quickly than that of PUR-3 upon cis → trans thermal isomerization after the end of irradiation, 0.45 and 0.14 s^{-1} being the fastest isomerization rates for PUR-1 and PUR-3, respectively (see Table 1). This table also shows that the cis → trans thermal isomerization proceeds with faster rates for PUR-1 and -2 versus PUR-3 and -4 and the rates of polymers with the same electron-withdrawing groups are similar.

For explaining the dynamical behaviors of Figures 3−5, we recall the mechanism of photoorientation and discuss the effect of a long-living cis isomer on photoorientation dynamics.

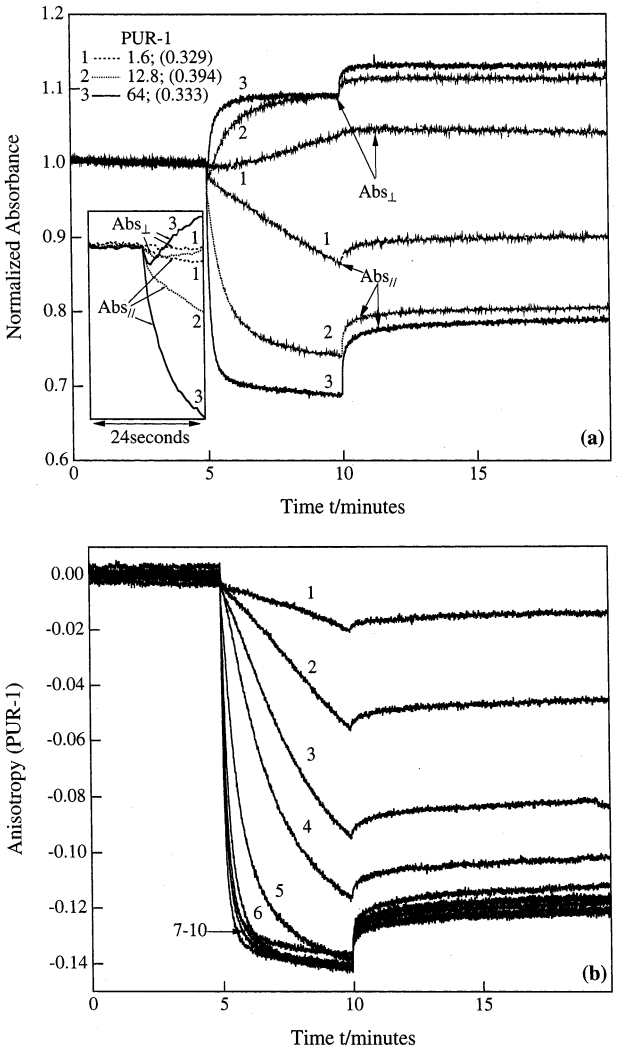

Figure 3. Photoorientation dynamics of PUR-1: (a) absorbance, normalized by the absorbance value prior to irradiation; (b) anisotropy. The irradiation light is turned on and off at 5 and 10 min, respectively. The numbers 1−3 in panel a and 1−10 in panel b indicate an increasing irradiation intensity the value of which is given in panel a in units of mW/cm^2 with the corresponding sample's absorbance prior to irradiation in units of OD (value in parentheses) and increases according to the series 0.8, 1.6, 3.2, 6.4, 12.8, 25.6, 38.4, 51.2, 64, and 76.8 mW/cm^2 in panel b. The inset shows an expanded view of the first few seconds of photoorientation.

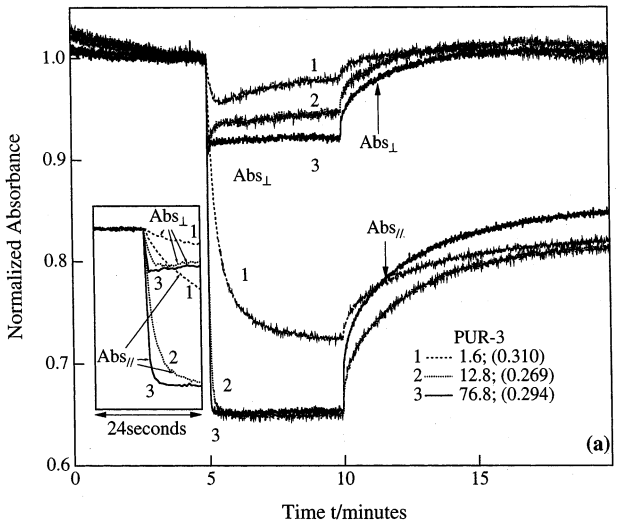

Figure 4. Photoorientation dynamics for PUR-3, absorbance normalized by the absorbance value prior to irradiation. The anisotropy showed a dynamical behavior (not shown) similar to that of Figure 3b. The irradiation intensity increased according to the series 0.2, 0.4, 0.8, 1.6, 3.2, 6.4, 12.8, 25.6, 38.4, 51.2, 64, and 76.8 mW/cm^2 (for clarity, only the data obtained by irradiation at 1.6, 12.8, and 76.8 mW/cm^2 are shown), and the sample OD prior to irradiation was ∼0.3.

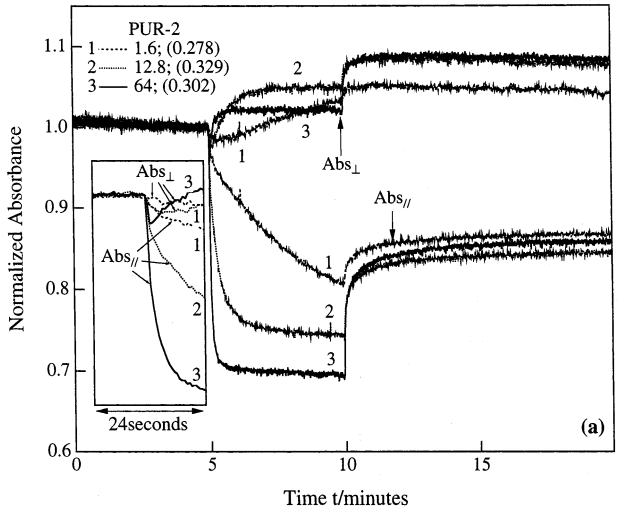

Figure 5. Photoorientation dynamics for PUR-2, absorbance normalized by the absorbance value prior to irradiation. The anisotropy showed a dynamical behavior (not shown) similar to that of Figure 3b. The irradiation intensity increased according to the series 0.8, 1.6, 3.2, 6.4, 12.8, 25.6, 38.4, 51.2, 64, and 76.8 mW/cm^2 (for clarity, only the data obtained by irradiation at 1.6, 12.8, and 64 mW/cm^2 are shown), and the sample OD prior to irradiation was ∼0.3.

Photoorientation by photoisomerization occurs through a polarization-sensitive photoexcitation, e.g., photoselection. The probability of exciting a transition dipole in an isomer is proportional to the cosine square of the angle between that transition dipole and the polarization of the excitation light. Transition dipoles that lie along the polarization of the irradiation light will be excited with the highest probability, and molecules may be isomerized and reoriented and may fade from the direction of the polarization of the irradiation light. As a consequence, the isomers, e.g., the transition dipoles that correspond to the irradiation wavelength, are eventually oriented into a direction that is perpendicular to the irradiation light polarization, and $Abs_\perp$ exceeds $Abs_\parallel$ for those transitions.

Two competing limiting cases of photoselection are worth discussing, namely, orientational hole burning (OHB) and pure photoorientation. If the chromophores are only photoisomerized through photoselection and they are not rotated, a large cis population is anisotropically generated and a hole is burned into the trans isomer orientational distribution (OHB). In this case, both $Abs_\parallel$ and $Abs_\perp$ change in the same direction with $(Abs_\parallel - Abs_0) = +3(Abs_\perp - Abs_0)$ at the beginning of the irradiation and $(Abs_\parallel - Abs_0) \approx (Abs_\perp - Abs_0)$ for hypothetically infinite irradiation intensities. Pure photoorientation occurs if the cis population is negligible and the trans isomer is rotated for each absorbed photon, a feature that has theoretical foundation.[54] These conditions imply higher reorientation rates and higher anisotropy values for higher irradiation intensities and a dynamical behavior in which $Abs_\parallel$ and $Abs_\perp$ evolve in opposite directions starting from the moment in which polarized light impinges the sample with $(Abs_\parallel - Abs_0) = -2(Abs_\perp - Abs_0)$; the factor -2, as well as the $+3$ above, originate from the orientational averaging of the chromophore's polarizability after photoselection. This dynamical behavior occurs nearly perfectly in PUR-1, with a small OHB dip at the beginning of irradiation

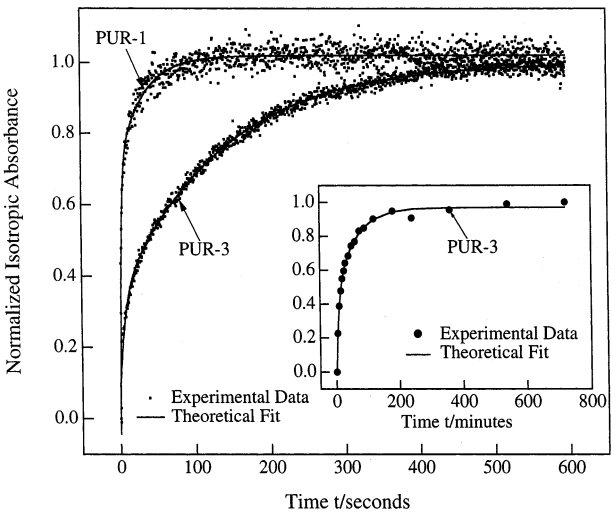

Figure 6. The first 600 s of the recovery of the isotropic absorbance of PUR-1 and PUR-3 after the irradiation light is turned off as observed by real-time dichroism. The theoretical fits are double exponential for the first 600 s and triple-exponential for the inset, e.g., for PUR-3 for the first 800 min. The absorbance is normalized as $(Abs - Abs_0)/(Abs_\infty - Abs_0)$, for which Abs is the time-dependent absorbance and Abs_0 and Abs_∞ are the initial, e.g., at the moment when the irradiation is turned off, and steady-state absorbances, respectively. The inset shows the recovery of the isotropic absorbance of PUR-3 as monitored by a UV−vis spectrophotometer. In the inset, the first data point was taken 1 min after irradiation.

TABLE 1: Rate Constants, k_i, and Weighting Coefficients, a_i, i = 1, 2, 3, of the cis → trans Thermal Isomerization of the Chromophore in Azo-PURs

	PUR-1	PUR-2	PUR-3	PUR-4
k_1 (s^{-1}); a_1	0.45; 0.75	0.41; 0.67	0.14; 0.18	0.27; 0.16
k_2 (s^{-1}); a_2	0.031; 0.31	0.024; 0.35	0.007; 0.47	0.01; 0.46
k_3 (s^{-1}); a_3			0.003; 0.30	0.0002; 0.40

(see Figure 3a). The chromophore in PUR-1 is, indeed, mostly in the trans form during photoorientation because of a photoisomerization quantum yield that is much higher in the backward, cis → trans, than in the forward, trans → cis, reaction (vide infra). In other words, the cis → trans thermal isomerization rate is faster than the pumping rate of the trans → cis photoisomerization, whereby the cis returns quickly to the trans isomer, yielding a negligible cis population during trans ↔ cis isomerization cycling.

To sum up the discussion about the differing dynamics of Figures 3−5, we infer that during photoorientation, both OHB and pure photoorientation decrease $Abs_{||}$, while pure photoorientation increases $Abs_\perp$ and OHB decreases it in a competing manner; all of the trends of Figures 3−5 can be explained by the competition scheme of OHB versus pure photoorientation. In PUR-3 and -4, OHB is dominant because of a long-living cis isomer (vide infra), and the increase, after sometime, of $Abs_\perp$ in PUR-3 is indicative of molecular reorientation following OHB. In PUR-2, near-pure photoorientation does not occur as clearly as it does in PUR-1 because of the differing polymer backbones of these two polymers (vide infra). In PUR-2, $Abs_\perp$ exceeds Abs_0, but not quite as it is the case for PUR-1.

Next, we discuss polymer structural effects on photoorientation in all azo-PURs. The effect of the structure of the polymer backbone on photoorientation can be also seen from the steady-state values of the photoinduced anisotropy. Figures 7 and 8, which have been obtained separately by two independent steady-state dichroism experiments, show that the level of induced anisotropy in all four azo-PURs is correlated to the

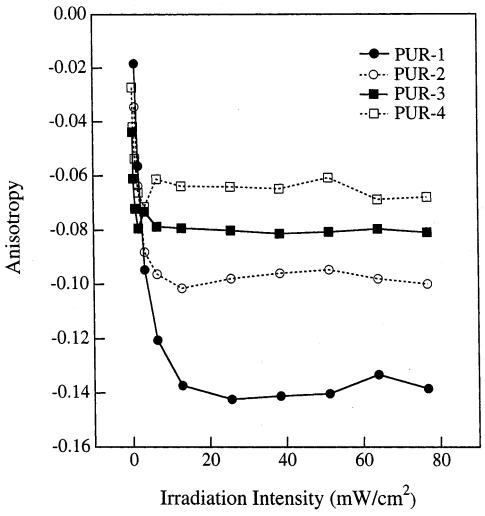

Figure 7. Photostationary state anisotropy in azo-PURs versus irradiation intensity. Each data point was taken after 5 min of irradiation. The data are those of real-time dichroism with 488 nm irradiation and analysis.

polymer structure. In Figure 7, we report the dichroic absorbance data obtained by linearly polarized 488 nm irradiation versus the irradiation intensity and analysis near the steady-state of irradiation. In Figure 8, we report the time dependence of the dichroic absorbance obtained after linearly polarized 488 nm irradiation and analysis at the maximum wavelength, for example, 470 nm for PUR-1 and -2, and 440 nm for PUR-3 and -4, measured by a UV−vis spectrophotometer. Figure 7 clearly shows a higher anisotropy for the photostationary state of PUR-1 versus that of PUR-2, -3, and -4. PUR-1 and PUR-2 have the same extinction coefficient at the analysis wavelength because they have the same azo chromophore; furthermore, the rate of the cis → trans thermal isomerization is nearly the same in both polymers. The seemingly small difference in the polymer backbone, e.g., the presence of the aromatic ring in the backbone of PUR-1, clearly influences the photoorientation efficiency for PUR-1 versus PUR-2. This aromatic versus aliphatic influence of the polymer backbone is also observed for PUR-3 versus PUR-4, confirming the influence of the polymer structure on photoorientation. Even though the observed anisotropy depends on the cis and trans balance in concentration and on the extinction coefficients of the isomers, as well as on the orientation of the isomers, polymers with the same chromophore but different backbones exhibit different levels of induced anisotropy under the same irradiation conditions according to the series PUR-1 > PUR-2 and PUR-3 > PUR-4. Figure 8 confirms the findings of Figure 7, and both Figures 7 and 8 demonstrate the fast cis → trans thermal isomerization and that the presence of the aromatic ring in the polymer backbone facilitates the photoorientation of the chromophore.

Now, we show that the spontaneous, thermally activated relaxation of the chromophores is primarily governed by the movement of the polymer backbone and not by the movement of the chromophore. To do so, we have recorded the erasure of the anisotropy, which is indicative of chromophore disorientation, in each polymer versus temperature (see Figure 9). The data in Figure 9 were obtained by heating an all-trans photooriented sample, e.g., a sample that was photooriented to the photostationary state and relaxed in the dark for 5 h to complete the cis → trans thermal isomerization, in the oven for 15 min at a given temperature. Then, we immediately recorded $Abs_{||}$ and $Abs_\perp$ from which we computed the anisotropy, and the measurement at the next temperature value followed. The

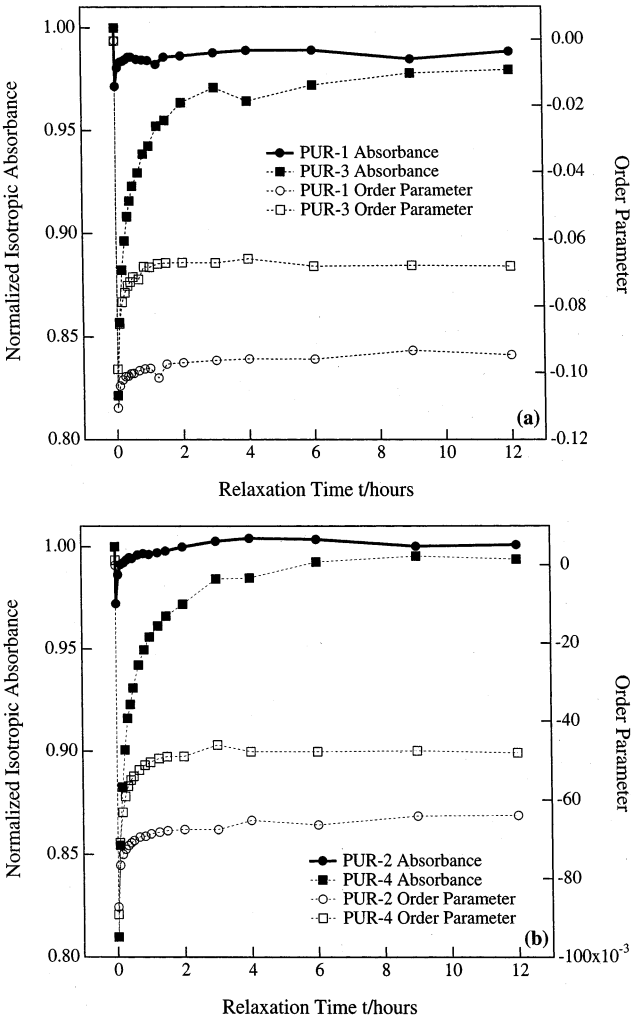

Figure 8. Isotropic absorbance and order parameter of (a) PUR-1 and -3 and (b) PUR-2 and -4 versus time after the end of 488 nm irradiation measured at the maximum absorption wavelength of PUR-1 and -3, for example, 470 and 440 nm, respectively. The first data point was taken before irradiation, and the second point was taken 1 min after irradiation. For the isotropic absorbance, the data points are normalized by the value of the absorbance before irradiation. Note the quick recovery of the absorbance after irradiation for PUR-1 and -2 versus PUR-3 and -4, indicative of a high thermal azo isomerization rate for the chromophore with the nitro electron-withdrawing group. The observed photoinduced orientation is quasi-permanent for all polymers.

initial isotropic absorbance of the sample remained unchanged on heating. It is clear from Figure 9 that polymers with the same backbone follow the same path independent from the chromophore, a feature that shows that the thermally activated orientational relaxation of the chromophores is primarily governed by the polymer backbone rather than the chromophore itself. This orientational relaxation is especially pronounced near the T_g of the polymers at which substantial spontaneous molecular movement occurs. Note that the T_g's of the azo-PURs that have the same backbone and different chromophores are slightly but noticeably different (140 versus 136 °C). Next, we quantify coupled photoisomerization and photoorientation in all four azo-PURs.

IV. Photoisomerization and Photoorientation Quantification in Azo-PURs

To quantify photoorientation by photoisomerization in A ↔ B photoisomerizable systems where B is unknown, which is the case of azo-PURs, it is necessary to develop an analytical

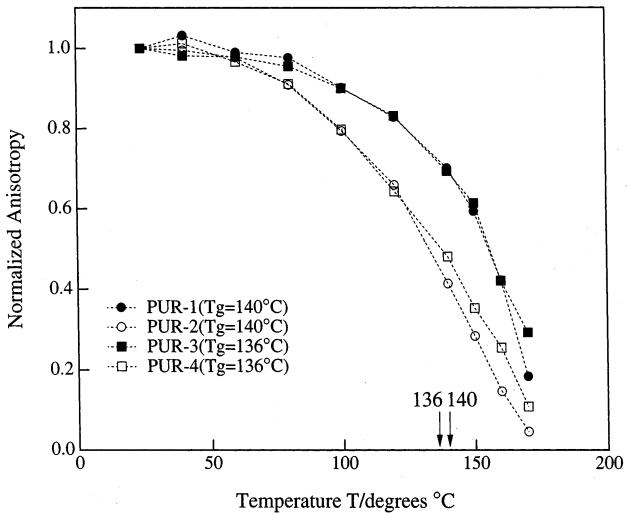

Figure 9. Erasure of the anisotropy versus temperature for azo-PURs. The data points are normalized by the value of the anisotropy at 20 °C. The polymers T_g's are indicated.

theory for comparison with experimental data. This theoretical development is given in detail in the Appendix, and in this section, we will give only the theoretical relations, for example, eqs 1−3, which will be used to measure coupled photoorientation and photoisomerization parameters.

$$p(\Delta) = 1000 I_0' (1 - 10^{-A_0'}) \phi'_{AB} (\epsilon_B - \epsilon_A) \quad (1)$$

$$p(\Delta A) = \frac{6}{5} 1000 I_0' (1 - 10^{-A_0'}) \phi'_{AB} (Q\epsilon_B - \epsilon_A) \quad (2)$$

$$1/S = -\frac{13}{2} - \frac{k}{\epsilon'_B \phi'_{BA} F'} \quad (3)$$

Equations 1 and 2 give, as a function of the incident irradiation light intensity, I_0', the slopes, $p(\Delta)$ and $p(\Delta A)$, of the time change of the isotropic absorbance and of the anisotropy at the early stage of photoorientation, respectively; eq 3 gives the order parameter, S, at the stationary state of photoorientation, also as a function of the irradiation light intensity through F', which is proportional to I_0' (see the Appendix). ϕ'_{AB} and ϕ'_{BA} are the quantum yields of the trans → cis and cis → trans photoisomerizations, respectively; ϵ_A and ϵ_B are the extinction coefficients of the trans and cis isomers, respectively; k is the rate of the cis → trans thermal isomerization, and it is equal to the reciprocal of the lifetime of isomer B (τ_B); A_0' is the absorbance of the sample measured at the irradiation wavelength prior to irradiation, and Q is a parameter that characterizes the change of the chromophore orientation after isomerization. For all of the azo-PURs, the experimentally observed slopes at the early time of photoorientation, $p(\Delta)$ and $p(\Delta A)$, exhibit a linear dependence on the irradiation light intensity (Figure 10), in agreement with eqs 1 and 2, and the photostationary state order parameter behaves according to eq 3, for example, $1/S$ obtained at the steady-state of irradiation induced A ↔ B orientation showed a linear dependence on the reciprocal of the irradiation light intensity (Figure 11). The fits by eqs 1−3 yielded ϕ_{AB}^{488}, ϕ_{BA}^{488}, and Q for all polymers, and their values are summarized in Table 2.

When the irradiation intensity is extrapolated to infinity, the experimentally observed order parameter for all azo-PURs is near −2/13; a value which is predicted by eq 3 and which we refer to as the *photoorientation constant*, or the constant of

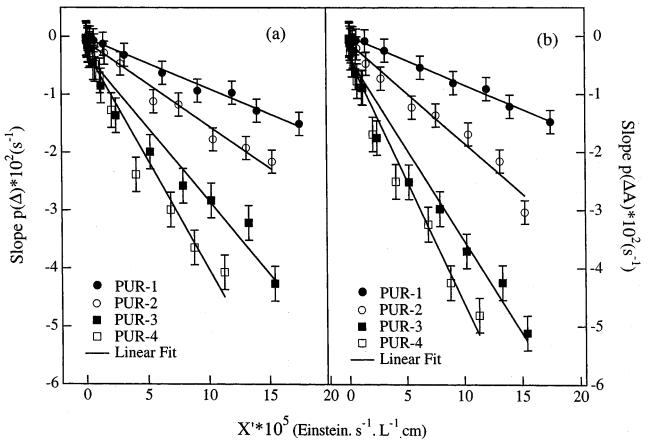

Figure 10. The fitted slopes $p(\Delta)$ and $p(\Delta A)$ of the observed early time evolution of the (a) isotropic absorbance and (b) anisotropy, respectively. The scatters are experimental data points, and the full lines are linear theoretical fits to eqs 1 and 2. $X' = F'A_0'$.

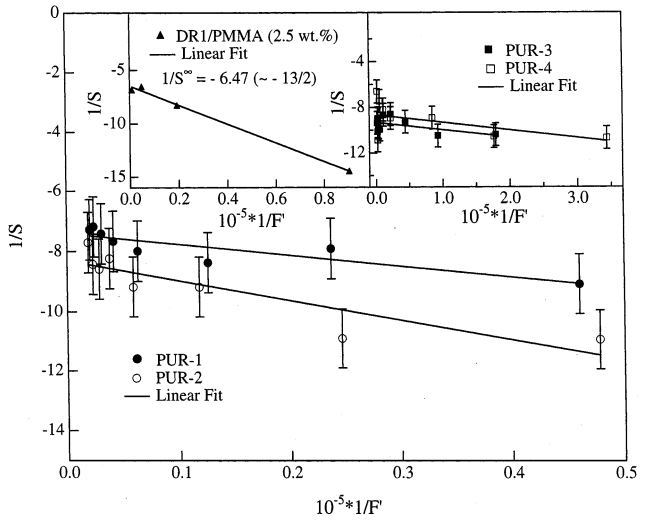

Figure 11. The reciprocal of the order parameter versus the reciprocal of the irradiation intensity for PUR-1 and -2. The scatters are experimental data points and the full lines are linear theoretical fits to eq 3. The insets show this dependence for PUR-3 and -4 and DR1/PMMA as adapted from ref 55.

TABLE 2: Coupled Photoisomerization and Photoorientation Parameters for Azo-PURs[a]

azo-PUR	ϵ_A^{488}	ϵ_B^{488}	ϕ_{AB}^{488}	ϕ_{BA}^{488}	Q^{488}
PUR-1	41 300	21 200	0.004 ± 0.002	0.57 ± 0.20	1.19 ± 0.02
PUR-2	41 300	21 200	0.007 ± 0.002	0.29 ± 0.05	1.01 ± 0.04
PUR-3	28 000	5 143	0.011 ± 0.001	0.21 ± 0.17	0.81 ± 0.05
PUR-4	28 000	5 143	0.017 ± 0.001	0.29 ± 0.20	1.37 ± 0.07

[a] The extinction coefficients are in units of L mol^{-1} cm^{-1}. The explanation of the different parameters is given in text.

photoorientation by photoisomerization. This value, for example, $-2/13$, sets the maximum orientation that can be achieved by photoisomerization and rationalizes, at least for high irradiation intensities, the concept of a uniform stationary-state molecular order for both the cis and trans isomers. Equation 3 was derived by assuming that the geometrical order parameters of the trans and cis orientational distributions are the same at the steady state of photoorientation (see Appendix). Amorphous azo-polymers should exhibit a photostationary state order parameter at infinite irradiation flux that is near the photoorientation constant. A good example from the literature is provided by disperse red one (DR1) molecules introduced as guests into films of PMMA.[55] In ref 55, both the anisotropy and the isotropic absorbance were measured as a function of the irradiating intensity, and the order parameter that is adapted from those measurements and that is shown as an inset to Figure 11 also exhibits an infinite flux value of S near $-2/13$. Even though in ref 55 the analysis wavelength, e.g., 514 nm, was different from the irradiation wavelength, e.g., 488 nm, these wavelengths are close enough within the same absorption band of the DR1 chromophore.

For photoisomerization and photoorientation parameters evaluation, ϵ_A and ϵ_B should be known. We have calculated ϵ_A from the absorption spectrum of the polymer solution before irradiation, assuming the same extinction coefficient in the film and in solution, and we have determined ϵ_B by the method of Fisher[19] modified by Rau et al.,[20] which holds not only for isotropic but also for anisotropic samples when the isotropic absorbance is considered (see Appendix). For this determination, we have recorded the isotropic absorbance change versus the irradiating light intensity, and we have extracted the sample absorbance change for an irradiation flux extrapolated to infinity for three different combinations of irradiation and analysis wavelengths, e.g., 488−488, 532−488, and 532−532 nm, irradiation and analysis, respectively. These experiments have been done by recording the transmitted light of a probe that is propagating perpendicular to the sample and polarized at the magic angle, e.g., ∼54.7°, from the vertically polarized pump, so anisotropy contributions to absorption changes are eliminated. The extent of cis concentration, e.g., the α value ($C_B = \alpha C$, C being the total concentration of both isomers and C_B the concentration of the B isomer), which we found at 488 nm for PUR-1 and -3, is 0.158 and 0.077, respectively. The obtained extinction coefficients are summarized in Table 2 together with the photochemical and photoorientation parameters.

For all four azo-PURs, the quantum yields of the forward, e.g., trans → cis, photoisomerization are much smaller than those of the backward, e.g., cis → trans, photoisomerization, a feature that shows that the azo-chromophores in those polymers are often in the trans form during trans ↔ cis cycling inasmuch as the rate of the cis → trans thermal back reaction is fast. For PUR-1, trans isomerizes to cis about 4 times for every 1000 photons absorbed, and once in the cis, it isomerizes back to the trans for only about 2 absorbed photons; in addition, the rate of cis → trans thermal isomerization is quite high, e.g., 0.45 s^{-1} for the fastest component. Here too it can be seen that the structure of the polymer influences photoorientation because the values of the quantum yields and the thermal isomerization rates are quite close for PUR-1 and PUR-2 and near-pure photoorientation is unambiguously observed only in PUR-1.

$Q \approx 1$ shows that upon isomerization the azo-chromophore rotates in a manner to maximize molecular nonpolar orientation during isomerization, in other words, maximize the second-order Legendre polynomial, e.g., the second moment of the distribution of the isomeric reorientation (see Appendix). $Q \approx 1$ also shows that the chromophore retains full memory of its orientation prior to isomerization and does not thermalize its orientation in excited states on photon absorption; otherwise, $Q \approx 0$. The fact that the azo chromophore moves, e.g., rotates, and retains full orientational memory after isomerization dictates that it must reorient by a well-defined angle upon isomerization. Such a change in the orientation of the chromophore's transition dipole after isomerization can be explained by the change in the shape of the chromophore, which is imposed by the isomerization reaction.

V. Conclusion

We have observed near-pure photoorientation of azo dye in an azo-polyurethane polymer, and we have studied the photoorientation movement of a series of azo-polyurethanes, each with distinct differences in the molecular structure of the unit building blocks. Pure photoorientation occurs when the chromophore is most of the time in the trans state during cis ↔ trans isomerization cycling, and it is influenced by the polymer structure, as well as by the photoisomerization quantum yields and the cis → trans thermal isomerization rate. We have also introduced the analytical theoretical equations that allow for the quantification of coupled photoisomerization and photoorientation of spectrally overlapping isomers. In particular, we have shown how photoisomerization quantum yields can be determined in anisotropic polymer films, and we have quantified the photoorientation movement of azo dye in azo-PURs. In these polymers, the reorientation of the transition dipole is due to the isomeric change in shape of the chromophore, and the movement of the isomers is not thermalized during isomerization. Photoorientation by photoisomerization can now be quantified thereby providing deep insight into chromophore (re)orientation.

Acknowledgment. The authors acknowledge support from the Japan Society for the Promotion of Science under the Research for the Future Program.

Appendix

Analytical Theory and Quantification of Photoorientation in A ↔ B Photoisomerizable Systems Where B is Unknown: Determination of Photoorientation Parameters and Photoisomerization Quantum Yields in Anisotropic Samples. Even though a phenomenological theory was developed for photoisomerization-induced molecular orientation few years ago,[54,55] bridges were yet to be set between photochemistry and nonlinear optics, in that tools to quantify coupled photoorientation and photoisomerization were yet to be developed. Recently, we have introduced the analytical theory that allows for the quantification of coupled photoisomerization and photoorientation in A ↔ B photoisomerizable systems where B is unknown, and we have used it to study quantitatively both the photoisomerization and photoorientation of photochromic spectrally distinguishable isomers in polymer films.[21,22] The quantification of photoorientation by photoisomerization can be done also for spectrally overlapping isomers, such as the cis and trans isomers of DR1, in the same manner that it is done for individualizable isomers. Indeed, in this appendix, we adapt the analytical theory of photoorientation by photoisomerization[21] to the case of spectrally overlapping isomers, and we develop analytical relations that describe the early time evolution and the steady state of photoorientation. For the sake of clarity, we recall the phenomenological equations of photoorientation within the purely polarized transitions framework. The principle and mechanism of photoorientation is discussed in detail in the text. In this appendix, we will discuss in succession purely polarized transitions and the general equations of photoorientation and the early time evolution and the stationary state of photoorientation and Fisher's method for anisotropic samples together with the analysis of photoorientation at a wavelength that is different from the irradiation wavelength.

Purely Polarized Transitions. In A ↔ B photoisomerization, light produces isomerization in both A → B and B → A directions, and spontaneous thermal isomerization proceeds generally in the backward B → A direction. In the following, A and B refer to the trans and cis isomers, respectively. We assume that A ↔ B photoconversion occurs upon excitation of a purely polarized transition with light linearly polarized along the laboratory axis *Z*, and we define a site-fixed right-handed orthogonal system of axes for each of the isomers A and B in which the molecule can exist, such that the angle between the Z_A and Z_B axes is χ. In isomers A and B, the electric dipole moments M_A^{UV} and M_B^{UV} responsible for excitation of a photochemical transition, say an ultraviolet (UV) transition, at a given irradiation wavelength are along the Z_A and Z_B axes, respectively, and when the chromophore isomerizes, the transition at the irradiation wavelength changes from Z_A to Z_B, or the inverse, depending on whether the isomerization is in the trans → cis or the cis → trans direction. In isomer B, the electric dipole moment M_B^{vis} responsible for excitation of a different photochemical transition, say a visible transition, at a given irradiation wavelength is at an angle labeled ω with respect to the Z_B axis and lies in the plane that contains the latter and bisects the angle between X_B and Y_B (Figure 12). For each of the isomers A and B, any polarized transition can be represented in the isomer's fixed molecular coordinates by an inclination angle, say ω for simplicity, with respect to a reference transition that is rigidly fixed to the molecular coordinates, say the transition that corresponds to the irradiation wavelength, in the same manner as the UV and vis transitions are represented for the B isomer in Figure 12. For each of the A and B isomers, the isotropic absorbance, $\overline{A_{A,B}} = (\mathrm{Abs}_{||}^{A,B} + 2\mathrm{Abs}_{\perp}^{A,B})/3$, the anisotropy, $\Delta A_{A,B} = \mathrm{Abs}_{||}^{A,B} - \mathrm{Abs}_{\perp}^{A,B}$, and the optical order parameter, $S_{A,B} = \Delta A_{A,B}/(3\overline{A_{A,B}})$, are given by

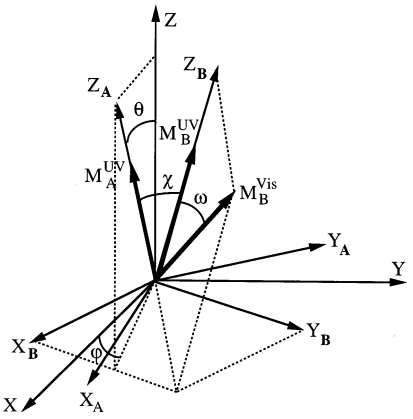

Figure 12. Schematic of axes and angles. *X*, *Y*, and *Z* indicate the laboratory coordinates axes, and $X_{A,B}$, $Y_{A,B}$, and $Z_{A,B}$ indicate the fixed molecular coordinates axes of the isomer. The angles θ, φ, χ, and ω and the transition electric dipole moments M_A^{UV}, M_B^{UV}, and M_B^{vis} are as defined in the text.

$$\overline{A_{A,B}} = \epsilon_{A,B} C_{A,B}$$

$$\Delta A_{A,B} = 3\epsilon_{A,B} P_2(\cos \omega_{A,B}) C_{A,B} A_2^{A,B}$$

$$S_{A,B} = P_2(\cos \omega_{A,B}) A_2^{A,B} \qquad \text{(A1)}$$

where $A_2^{A,B}$ is the isomer's geometrical order parameter; it is independent of the spectral properties of the chromophore, and $P_2(\cos \omega_{A,B})$ is the second-order Legendre polynomial of cos $\omega_{A,B}$ given by

$$P_2(\cos \omega_{A,B}) = (3 \cos^2 \omega_{A,B} - 1)/2 \qquad \text{(A2)}$$

$\omega_{A,B}$ being the angle that defines the orientation of a transition that corresponds to the analysis wavelength versus the irradiation

wavelength transition. In other words, if analysis is done at the irradiation wavelength, $\omega_{A,B} = 0$ and $P_2(\cos \omega_{A,B}) = 1$. $Abs_{||}^{A,B}$ and $Abs_{\perp}^{A,B}$ stand for absorption of light polarized parallel and perpendicular to the polarization of the irradiation light, respectively. We represent by C_A and C_B and ϵ_A^λ and ϵ_B^λ the concentrations and the isotropic extinction coefficients, for example, those coefficients that can be measured from the isotropic absorbance spectra, of the isomers A and B, respectively. $\epsilon_{A,B}^\lambda$ is proportional to $|M_{A,B}^\lambda|^2$. For all the equations, the sub- and superscripts A and B, if any, refer to the isomers A and B, respectively.

General Equations of Photoorientation. The time-dependent expression of photoorientation is derived by considering the elementary contribution per unit time to the orientation by the fraction of the molecules, $dC_{A,B}(\Omega)$, of which the representative moment of transition is present in the elementary solid angle, $d\Omega$, near the direction $\Omega(\theta,\varphi)$ relative to the fixed laboratory axes (Figure 12). This elementary contribution results from orientational hole burning and orientational redistribution and rotational diffusion. The transitions are assumed to be purely polarized, and the irradiation light polarization is along the Z axis. The elementary contribution to photoorientation is given by

$$\frac{dC_A(\Omega)}{dt} = -3F'\phi'_{AB}\epsilon'_A \cos^2\theta\, C_A(\Omega) + 3F'\phi'_{BA}\epsilon'_B \int_{\Omega'} C_B(\Omega') \cos^2\theta'\, P^{BA}(\Omega' \rightarrow \Omega)\, d\Omega' + \frac{1}{\tau_B}\int_{\Omega'} C_B(\Omega') Q(\Omega' \rightarrow \Omega)\, d\Omega' + D_A \mathscr{R}\left[\mathscr{R} C_A(\Omega) + C_A(\Omega)\mathscr{R}\frac{U_A}{kT}\right]$$

$$\frac{dC_B(\Omega)}{dt} = -3F'\phi'_{BA}\epsilon'_B \cos^2\theta\, C_B(\Omega) + 3F'\phi'_{AB}\epsilon'_A \int_{\Omega'} C_A(\Omega') \cos^2\theta'\, P^{AB}(\Omega' \rightarrow \Omega)\, d\Omega' - \frac{1}{\tau_B} C_B(\Omega') + D_B \mathscr{R}\left[\mathscr{R} C_B(\Omega) + C_B(\Omega)\mathscr{R}\frac{U_B}{kT}\right] \quad \text{(A3)}$$

$P^{AB}(\Omega' \rightarrow \Omega)$, $P^{BA}(\Omega' \rightarrow \Omega)$, and $Q(\Omega' \rightarrow \Omega)$ are the probabilities that the electric transition dipole moment of the chromophore will rotate in the A → B and B → A photoisomerizations and B → A thermal isomerization, respectively. The orientational hole burning is represented by a probability proportional to $\cos^2\theta$, and the last term in each of the equations above describes the rotational diffusion that is due to Brownian motion. The latter is a Smoluchowski equation for the rotational diffusion characterized by a constant of diffusion D_A and D_B for the A and B isomers, respectively, where $\mathscr{R}$ is the rotational operator. k is the Boltzmann constant, T is the absolute temperature, and $U_{A,B}$ is an interaction energy to which the isomers can be subjected. Depending on the type of interaction, $U_{A,B}$ can be polar or nonpolar. It is polar when the chromophores are isomerized in the presence of an electric field (the so-called photoassisted poling, the theory of which was discussed in detail elsewhere[55]) and nonpolar when intermolecular interactions, such as liquid crystalline-type interactions, are present. We do not discuss these two cases, and we consider the case of $U_{A,B} = 0$ where friction is the only constraint additional to isomerization. F' is a factor that takes into account that only some part of the totally absorbed amount of light induces photoreaction. F' is given by[56]

$$F' = \frac{1000(1 - 10^{-A'_0})}{A'_0} I'_0. \quad \text{(A4)}$$

The knowledge of the amount of absorbed light is prerequisite for photoreaction quantification, and even though F' is derived for stirred solutions from the Lambert−Beer's law that stipulates that the irradiation intensity decays exponentially along the optical path through the sample, it certainly takes into account the attenuation of the irradiation intensity due to the sample absorption, and it provides a simple tool for a good estimation the amount of absorbed light by films of polymer.[7,20] The factor 1000 occurs when the intensity of the irradiating light (flux of photons per square centimeter) is expressed in einstein s^{-1} L^{-1} cm. We adopt some of the notations and units that are used in photochemistry because, in particular, quantum yield measurements are considered. The primed quantities refer to an analysis at the irradiation wavelength, and the unprimed ones refer to an arbitrary analysis wavelength. I'_0 is the incident flux of photons per square centimeter; A'_0 is the sample absorbance prior to irradiation. The normalizations are

$$\int_\Omega C_A(\Omega)\, d\Omega = C_A; \quad \int_\Omega C_B(\Omega)\, d\Omega = C_B; \quad C_A + C_B = C \quad \text{(A5)}$$

where C is the total concentration of the chromophores. With bulk azimuthal symmetry, the symmetry axis is the Z axis, for example, the direction of the polarization of the irradiation light; the statistical molecular orientation for each of the photooriented A and B isomers is described by an orientational distribution function $G_{A,B}(\theta)$ that depends only on the polar angle, and it can be expressed in the standard basis of Legendre polynomials, $P_n(\cos\theta)$, with $A_n^{A,B}$ as expansion coefficients (order parameters) of order n (integer). $C_{A,B}(\Omega)$ is given by

$$C_{A,B}(\Omega) = C_{A,B} G_{A,B}(\theta)$$

with

$$G_{A,B}(\theta) = \frac{1}{2\pi}\sum_{n=0}^{\infty} \frac{2n+1}{2} A_n^{A,B} P_n(\cos\theta)$$

and

$$A_n^{A,B} = \int_0^\pi G_{A,B}(\theta) P_n(\cos\theta) \sin\theta\, d\theta$$

and

$$A_0^{A,B} = 1 \quad \text{(A6)}$$

The redistribution processes, $P^{AB}(\Omega' \rightarrow \Omega)$ and $P^{BA}(\Omega' \rightarrow \Omega)$ and $Q(\Omega' \rightarrow \Omega)$, depend only on the rotation angle χ between Ω and Ω', and they can also be expressed in terms of Legendre polynomials with $P_n^{A \rightarrow B}$ and $P_n^{B \rightarrow A}$ and $Q_n^{B \rightarrow A}$ as expansion parameters, respectively. These parameters characterize the orientational memory of the molecules after the A → B and B → A photoisomerization reactions and B → A thermal isomerization.

$$P^{AB}(\chi) = \frac{1}{2\pi}\sum_{q=0}^{\infty}\frac{2q+1}{2}P_q^{A\to B}P_q(\cos\chi)$$

$$P^{BA}(\chi) = \frac{1}{2\pi}\sum_{q=0}^{\infty}\frac{2q+1}{2}P_q^{B\to A}P_q(\cos\chi)$$

$$Q(\chi) = \frac{1}{2\pi}\sum_{m=2}^{\infty}\frac{2m+1}{2}Q_m^{B\to A}P_m(\cos\chi)$$

with

$$P_0^{A\to B} = P_0^{B\to A} = Q_0^{B\to A} = 1 \qquad \text{(A7)}$$

When Legendre formalism is used, the variations of the cis and trans orientational distributions are given by the variations of their expansion parameters, for example, $C_n^{A,B} = C_{A,B}A_n^{A,B}$. Indeed, by substitution of eqs A4−A6 into eq A3 and use of the orthogonality as well as recurrence equations of Legendre polynomials, the general rate equations, for example, eq A3, resume to the system of equations given by eq A8.

$$\frac{dC_{A,n}}{dt} = -3F'\phi'_{AB}\epsilon'_A\{C_A\} + 3F'\phi'_{BA}\epsilon'_B P_n^{B\to A}\{C_B\} + kQ_n^{B\to A}C_{B,n} - n(n+1)D_A C_{A,n}$$

$$\frac{dC_{B,n}}{dt} = 3F'\phi'_{AB}\epsilon'_A P_n^{A\to B}\{C_A\} - 3F'\phi'_{BA}\epsilon'_B\{C_B\} - kQ_n^{B\to A}C_{B,n} - n(n+1)D_A C_{B,n}$$

where

$$\{C_A\} = \{\kappa_{n+}C_{A,n+2} + \kappa_n C_{A,n} + \kappa_{n-}C_{A,n-2}\}$$
$$\{C_B\} = \{\kappa_{n+}C_{B,n+2} + \kappa_n C_{B,n} + \kappa_{n-}C_{B,n-2}\} \qquad \text{(A8)}$$

and

$$\kappa_{n+} = \frac{(n+1)(n+2)}{(2n+1)(2n+3)}, \quad \kappa_n = \frac{2n^2+2n-1}{(2n-1)(2n+3)}, \quad \text{and} \quad \kappa_{n-} = \frac{n(n-1)}{(2n-1)(2n+1)}$$

This system of equations shows that polarized light irradiation creates anisotropy and photoorientation by photoisomerization through even orders. A solution to the time evolution of the cis and trans expansion parameters cannot be found without approximations, and this is when physics comes into play. Approximate numerical simulations are possible. We show that for rigorous comparison of experimental data with the photoorientation theory, it is not necessary to find a solution for the dynamics, even in the most general case in which there is not enough room for approximations, for example, that of push−pull azo dyes, such as DR1, because of the strong overlap of the linear absorption spectra of the cis and trans isomers of such chromophores. Rigorous analytical expressions of the steady-state behavior and the early time evolution provide the necessary tool for a full characterization of photoorientation by photoisomerization.

Early Time Evolution of Photoorientation. At the early time evolution, the cis concentration is negligibly small, and if we introduce the extent, α, of the concentration of isomer B, for example, $C_B = \alpha C$ and $C_A = (1-\alpha)C$, we obtain the following equation by setting $n = 0$ in system A8.

$$\frac{d\alpha}{dt} = F'\epsilon'_A\phi'_{AB}(1 + 2A_{2A}) \qquad \text{(A9)}$$

A_{2A} must be determined to find the expression of α. The following two equations, which are derived from system A8 for the early time evolution, for example, for $\alpha \ll 1$, allow for the determination of A_{2A}.

$$\frac{dC_{A,n}}{dt} = -3F'\phi'_{AB}\epsilon'_A\{C_A\} - n(n+1)D_A C_{A,n} \qquad \text{(A10)}$$

$$\frac{dC_{A,n}}{dt} = -\frac{1}{P_n^{A\to B}}\frac{dC_{B,n}}{dt} - n(n+1)D_A C_{A,n} \qquad \text{(A11)}$$

Setting $n = 2$ in eq A10 yields the second- and fourth-order parameters of the trans distribution, which are linear functions of the time, t. These are given by

$$A_{2A} = -\frac{2}{5}F'\epsilon'_A\phi'_{AB}t \quad \text{and} \quad A_{4A} = \left(\frac{11}{18}F'\epsilon'_A\phi'_{AB} + \frac{7}{3}D_A\right)t \qquad \text{(A12)}$$

where t represents the time. With substitution of A_{2A} in eq A9 and notation that at the early time evolution $t^2 \ll t$, eq A9 yields

$$\alpha = F'\epsilon'_A\phi'_{AB}t \qquad \text{(A13)}$$

At a given analysis wavelength, the absorption change, $\Delta = A - A_A$, is given by

$$\Delta = \alpha C(\epsilon_B - \epsilon_A) \qquad \text{(A14)}$$

where $A_A = \epsilon_A C$ and A are the sample absorbances before and during irradiation, respectively. Note that the sample is all-trans prior to irradiation. Substituting eq A13 into eq A14 yields

$$\Delta = 1000I'_0(1 - 10^{-A'_0})\phi'_{AB}(\epsilon_B - \epsilon_A)t \qquad \text{(A15)}$$

which is the absorbance change at the early time evolution of photoorientation, the slope of which is given by

$$p(\Delta) = 1000I'_0(1 - 10^{-A'_0})\phi'_{AB}(\epsilon_B - \epsilon_A) \qquad \text{(A16)}$$

For the anisotropy change, we set $n = 2$ in eq A11 and solve for αA_{2B} with $t^2 \ll t$ in mind, and we have

$$\alpha A_{2B} = \frac{2}{5}P_2^{A\to B}F'\epsilon'_A\phi'_{AB}t \qquad \text{(A17)}$$

and

$$A_{2B} = \frac{2}{5}P_2^{A\to B} \qquad \text{(A18)}$$

The total anisotropy, $\Delta A = \Delta A_A + \Delta A_B$, is derived by summing the anisotropies due to the orientation of both isomers, for example, $\Delta A_{A,B} = 3C\epsilon_{A,B}P_2(\cos\omega_{A,B})A_{2A,2B}$, and by using eqs A17 and A18. ΔA reads

$$\Delta A = \frac{6}{5}1000I'_0(1 - 10^{-A'_0})\phi'_{AB}\{P_2^{A\to B}P_2(\cos\omega_B)\epsilon_B - P_2(\cos\omega_A)\epsilon_A\}t \qquad \text{(A19)}$$

$P_2(\cos\omega_{A,B})$ is the second-order Legendre polynomial of cos

$\omega_{A,B}$, and $\omega_{A,B}$ is the angle between the irradiation and analysis transition moments of the A,B isomer. If analysis is performed at the irradiation wavelength, $\omega_{A,B} = 0$ and $P_2(\cos \omega_{A,B}) = 1$, and the slope, $p(\Delta A)$, of ΔA resumes to

$$p(\Delta A) = \frac{6}{5} 1000 I'_0 (1 - 10^{-A'_0}) \phi'_{AB} (P_2^{A\rightarrow B} \epsilon_B - \epsilon_A) \qquad (A20)$$

In summary, the early stage of photoorientation by photoisomerization of spectrally overlapping isomers is described by eqs A15 and A19. In the text, we show how fits to experimental data by eqs A16 and A20 allow for the determination of ϕ'_{AB} and $P_2^{A\rightarrow B}$, which is replaced by Q in eq 1.

Steady-State Behavior. During the steady state of photoorientation, the expansion parameters $C_{A,n}$ and $C_{B,n}$ are constants, for example, $dC_{A,n}/dt = dC_{B,n}/dt = 0$, and if the first equation of the system of eq A8 is multiplied by $P_n^{A\rightarrow B}$ and added to the second equation of that system, the following relation, for example, eq A21, is obtained after rearrangement.

$$0 = 3\frac{F'}{k}\phi'_{BA}\epsilon'_B\{C_B\} + \frac{(P_n^{A\rightarrow B} Q_n^{B\rightarrow A} - 1) - k_D^B/k}{(P_n^{A\rightarrow B} P_n^{B\rightarrow A} - 1)} C_{B,n} - \frac{P_n^{A\rightarrow B} k_D^A/k}{(P_n^{A\rightarrow B} P_n^{B\rightarrow A} - 1)} C_{A,n} \qquad (A21)$$

where $k_D^{A,B} = n(n+1)D_{A,B}$ is the isomer's diffusion rate. Equation A21 is valid for $n \neq 0$, and it allows for the derivation of the steady-state order parameters of the isomers orientational distribution. Indeed, with the two following assumptions, eq A21 resumes to eq A22 for $n = 2$ after rearrangement: (i) The diffusion rates of both the A and B isomers, k_D^A and k_D^B, respectively, are negligibly small in comparison to the cis $\rightarrow$ trans thermal isomerization rate k. This is a good approximation to use when the chromophores are introduced into polymers because spontaneous molecular movement in polymeric materials is most efficient near the polymer T_g and strongly hindered far below it. In functionalized azo-polymers, photoorientation can be quasi-permanent at room temperature, a feature that is true for the azo-PURs studied (vide infra). (ii) The process of isomeric-type reorientation is assumed, e.g., that process in which the reorientation of the transition dipole is only due to the isomeric change in shape and in which the parameters, e.g., $P_n^{A\rightarrow B}$ and $P_n^{B\rightarrow A}$ and $Q_n^{B\rightarrow A}$, that describe the reorientation of the transition during the photoinduced and thermal isomerization reactions are equal, say equal to Q. Molecular orbital calculations show that the orientation of transition dipoles changes upon chromophore photoisomerization.[7,22]

$$\frac{36}{35}A_4^B + \left(\frac{11}{7} + \frac{k}{\epsilon'_B\phi'_{BA}}\frac{1}{F'}\right)A_2^B + \frac{2}{5} = 0 \qquad (A22)$$

The solution of eq A22 must be of the form

$$A_2^B = \frac{1}{x + \frac{k_2}{\epsilon'_B\phi'_{BA}}\frac{1}{F'}} \quad \text{and} \quad A_4^B = \left(1 + \frac{k_4}{\epsilon'_B\phi'_{BA}}\frac{1}{F'}\right)A_2^B \qquad (A23)$$

Because eq A22 is valid for any irradiation intensity, $x = -13/2$, and $2k_2/5 + 36k_4/35 = -k$. Rigorously, k_2 and k_4 are proportional to k, and $k_2 = -k$ is a physically reasonable solution. So,

$$\frac{1}{A_2^B} = -\frac{13}{2} - \frac{k}{\epsilon'_B\phi'_{BA}}\frac{1}{F'} \quad \text{and}$$

$$\frac{1}{S^B} = \frac{1}{P_2(\cos\omega_B)}\left(-\frac{13}{2} - \frac{k}{\epsilon'_B\phi'_{BA}}\frac{1}{F'}\right) \qquad (A24)$$

No truncation above any order has been made for the determination of A_2^B and S^B, and the solution given by eq A24 is certainly physical because it corresponds to actual observed behavior (vide infra). Equation A24 is useful when isomer B is spectrally distinguishable from isomer A, and it allows for the determination of $P_2(\cos \omega_B)$ by fitting eq A24 to experimental data as has been done for photooriented spiropyran and diarylethene derivatives in films of PMMA.[21,22] For spectrally overlapping isomers, the following equation, e.g., eq A25, gives the order parameters, e.g., the geometrical A_2 and spectral S, which characterize the orientational distribution of the whole, e.g., trans and cis, molecular distribution.

$$\frac{1}{S} = \frac{1}{A_2} = -\frac{13}{2} - \frac{k}{\epsilon'_B\phi'_{BA}}\frac{1}{F'} \qquad (A25)$$

Equation A25 assumes that the geometrical order parameters, A_2, of the orientational distribution of the cis and trans isomers are equal at the photostationary state of irradiation. This assumption physically mirrors a uniform molecular orientational distribution of both cis and trans isomers, and it simplifies considerably the expression of the photostationary state orientational order and provides a simple law for steady-state photoorientation characterization. This assumption is supported by the experimental finding of the photoorientation of all four azo-PURs and DR1 in PMMA. Equation A25 holds when analysis is performed at the irradiation wavelength, and fits by eq A25 allow for the measurement of ϕ'_{BA}. Inasmuch as measured values of $P_2(\cos \omega_B)$ can be rigorous because the value of $-13/2$ was derived without compromise, measured values of ϕ'_{BA} depend on the assumption $k_2 = -k$.

Irradiation and Analysis at Different Wavelengths. When the analysis of photoorientation is performed at a wavelength that is different from the irradiation wavelength, the respective orientation of the analysis and irradiation transition dipoles of both the cis and trans isomers can be found. Indeed, setting $n = 0$ in eq A8 yields the following relation for the photostationary state of irradiation:

$$\frac{\epsilon'_A\phi'_{AB}}{\epsilon'_B\phi'_{BA}}(1 + 2A_{2A}) = \frac{\alpha}{1-\alpha}\left\{(1 + 2A_{2B}) + \frac{k}{\epsilon'_B\phi'_{BA}F'}\right\} \qquad (A26)$$

In this equation, the trans and cis photostationary state order parameters, A_{2A} and A_{2B}, respectively, are given by eq A25. When the irradiation intensity, for example, F', is extrapolated to infinity, $A_{2A}^{\infty} = A_{2B}^{\infty} = A_2^{\infty} = -2/13$, eq A26 resumes to Fisher's stationary state relation for thermally irreversible systems:[19]

$$\frac{\epsilon'_A\phi'_{AB}}{\epsilon'_B\phi'_{BA}} = \frac{\alpha^{\infty}}{1-\alpha^{\infty}} \qquad (A27)$$

So, when photoorientation analysis is not performed at the irradiation wavelength, the order parameter at infinite irradiation intensity of spectrally overlapping isomers reads

$$S = -\frac{2}{13}\frac{P_2(\cos\omega_B) + aP_2(\cos\omega_A)}{1+a} \quad \text{with} \quad a = \frac{\epsilon_A}{\epsilon_B}\frac{\epsilon'_B\phi'_{BA}}{\epsilon'_A\phi'_{AB}} \qquad (A28)$$

$P_2(\cos\ \omega_A)$ and $P_2(\cos\ \omega_B)$ are the second-order Legendre polynomials of ω_A and ω_B, which are the angles between the irradiation and analysis transitions of isomers A and B, respectively. ω_A and ω_B can be experimentally determined by a two-step photoorientation experiment, for example, irradiate at a wavelength λ_1 and analyze at λ_2, and irradiate at λ_2 and analyze at λ_1. While S changes for each step, $P_2(\cos\ \omega_B)$ and $P_2(\cos\ \omega_A)$ remain unchanged, and their determination is straightforward. a can be determined before hand by determining the cis spectrum by the method of Fisher and the quantum yields by photoorientation analysis at the irradiation wavelength.

References and Notes

(1) *Photoreactive Organic Thin Films*; Sekkat, Z., Knoll, W., Eds.; Academic Press: San Diego, CA, 2002 and references therein.

(2) Delaire, J. A.; Nakatani, K. *Chem. Rev.* **2000**, *100* (5), 1817.

(3) Sekkat, Z.; Knoll, W. In *Advances in Photochemistry*; Neckers, D. C., Volman, D. H., Von Bunau, G., Eds.; Wiley and Sons: New York, 1997; Vol. 22, p 117. Sekkat, Z.; Knoll, W. *SPIE Proc.* **1997**, *2998*, 164. Sekkat, Z.; Knoesen, A.; Knoll, W.; Miller, R. D. In *SPIE Critical Reviews*; Najafi, I., Andrews, M. P., Eds.; SPIE—the International Society for Optical Engineering: Bellingham, WA, 1997; Vol. CR68, p 374. Sekkat, Z.; Knoesen, A.; Lee, V. Y.; Miller, R. D.; Wood, J.; Knoll, W. In *Organic Thin Films*; Frank, C. W., Ed.; ACS Symposium Series 695; American Chemical Society: Washington, DC, 1998, p 295.

(4) Sekkat, Z.; Kleideiter, G.; Knoll, W. *J. Opt. Soc. Am. B* **2001**, *18*, 1854.

(5) Tawa, K.; Kamada, K.; Kiyohara, K.; Ohta, K.; Yasumatsu, D.; Sekkat, Z.; Kawata, S. *Macromolecules* **2001**, *34*, 8232.

(6) Sekkat, Z.; Dumont, M. *Appl. Phys. B* **1992**, *54*, 486; *Mol. Cryst. Liq. Cryst. Sci. Technol., Sect. B* **1992**, *2*, 359; *SPIE Proc.* **1992**, *1774*, 188.

(7) Loucif-Saibi, R.; Nakatani, K.; Delaire, J. A.; Dumont, M.; Sekkat, Z. *Chem. Mater.* **1993**, *5*, 229.

(8) Palto, S. P.; Blinov, L. M.; Yudin, S. G.; Grewer, G.; Schönhoff, M.; Lösche, M. *Chem. Phys. Lett.* **1993**, *202*, 308.

(9) Blanchard, P. M.; Mitchell, G. R. *Appl. Phys. Lett.* **1993**, *63*, 2038.

(10) Charra, F.; Kajzar, F.; Nunzi, J. M.; Raimond, P.; Idiart, E. *Opt. Lett.* **1993**, *12*, 941.

(11) Sekkat, Z.; Dumont, M. *Appl. Phys. B* **1991**, *53*, 121.

(12) Shi, Y.; Steier, W. H.; Yu, L.; Shen, M.; Dalton, L. R. *Appl. Phys. Lett.* **1991**, *58*, 1131.

(13) Rochon, P.; Gosselin, J.; Natansohn, A.; Xie, S. *Appl. Phys. Lett.* **1992**, *60*, 4.

(14) Sekkat, Z.; Knoesen, A.; Lee, V. Y.; Miller, R. D. *J. Phys. Chem. B* **1997**, *101*, 4733.

(15) Neoport, B. S.; Stolbova, O. V. *Opt. Spectrosc.* **1961**, *10*, 146.

(16) Todorov, T.; Nicolova, L.; Tomova, T. *Appl. Opt.* **1984**, *23*, 4309.

(17) Thulstrup, E. W.; Michl, J. *J. Am. Chem. Soc.* **1982**, *104*, 5594.

(18) Zimmerman, G.; Chow, L. Y.; Paik, U. Y. *J. Am. Chem. Soc.* **1958**, *80*, 3528.

(19) Fisher, E. *J. Phys. Chem.* **1967**, *71*, 3704.

(20) Rau, H.; Greiner, G.; Gauglitz, G.; Meier, H. *J. Phys. Chem.* **1990**, *94*, 6523.

(21) Ishitobi, H.; Sekkat, Z.; Kawata, S. *Chem. Phys. Lett.* **2000**, *316*, 578.

(22) Ishitobi, H.; Sekkat, Z.; Kawata, S. *J. Am. Chem. Soc.* **2000**, *122*, 12802.

(23) Sekkat, Z.; Kang, C. S.; Aust, E. F.; Wegner, G.; Knoll, W. *Chem. Mater.* **1995**, *7*, 142. Sekkat, Z.; Wood, J.; Knoll, W. *J. Chem. Phys.* **1995**, *99*, 17226.

(24) Buffeteau, T.; Pézolet, M. *Appl. Spectrosc.* **1996**, *50*, 948.

(25) Böhm, N.; Materny, A.; Kiefer, W.; Steins, H.; Müller, M. M.; Schottner, G. *Macromolecules* **1996**, *29*, 2599.

(26) Eich, M.; Wendorff, J. H. *J. Opt. Soc. Am. B* **1990**, *7*, 1428.

(27) Anderle, K.; Birenheide, R.; Werner, M. J. A.; Wendorff, J. H. *Liq. Cryst.* **1991**, *9*, 691.

(28) Wiesner, U.; Reynolds, N.; Boeffel, C.; Spiess, W. H. *Liq. Cryst.* **1992**, *11*, 251.

(29) Hvilsed, S.; Andruzzi, F.; Ramanujam, R. *Opt. Lett.* **1992**, *17*, 1234.

(30) Lagugné Labarthet, F.; Sourisseau, C. *J. Raman Spectrosc.* **1996**, *27*, 491.

(31) Sawodny, M.; Schmidt, A.; Stamm, M.; Knoll, W.; Urban, C.; Ringsdorf, H. *Polym. Adv. Technol.* **1991**, *2*, 127.

(32) Büchel, M.; Sekkat, Z.; Paul, S.; Weichart, B.; Menzel, H.; Knoll, W. *Langmuir* **1995**, *11*, 4460.

(33) Stumpe, J.; Fischer, Th.; Menzel, H. *Macromolecules* **1996**, *29*, 2831.

(34) Wang, R.; Iyoda, T.; Hashimoto, K.; Fujishima, A. *J. Phys. Chem.* **1995**, *99*, 3352.

(35) Schönhoff, M.; Mertesdorf, M.; Lösche, M. *J. Phys. Chem.* **1996**, *100*, 7558.

(36) Seki, T.; Sakuragi, M.; Kawanishi, Y.; Suzuki, Y.; Tamaki, T.; Fukuda, R.; Ichimura, K. *Langmuir* **1993**, *9*, 211.

(37) Gibbons, W. M.; Shannon, P. J., Sun, S. T.; Sweltin, B. J. *Nature* **1991**, *95*, 509.

(38) Sekkat, Z.; Büchel, M.; Orendi, H.; Knobloch, H.; Seki, T.; Ito, S.; Koberstein, J.; Knoll, W. *Opt. Commun.* **1994**, *11*, 324.

(39) Ichimura, K.; Hayashi, Y.; Akiyama, H. *Langmuir* **1993**, *9*, 3298.

(40) Wolf, M. O.; Fox, M. A. *Langmuir* **1996**, *12*, 955.

(41) Sekkat, Z.; Wood, J.; Geerts, Y.; Knoll, W. *Langmuir* **1995**, *11*, 2856. Sekkat, Z.; Wood, J.; Geerts, Y.; Knoll, W. *Langmuir* **1996**, *12*, 2976.

(42) Junge, M.; McGrath, D. V. *Chem. Commun.* **1997**, *9*, 857.

(43) Song, X.; Geiger, C.; Vaday, S.; Perlstein, J.; Whitten, D. G. *J. Photochem. Photobiol. A: Chem.* **1996**, *102*, 39.

(44) Fissi, A.; Pieroni, O.; Balestreri, E.; Amato, C. *Macromolecules* **1996**, *29*, 4680.

(45) Berg, R. H.; Hvilsed, S.; Ramanujamm, P. S. *Nature* **1996**, *383*, 505.

(46) Hoffmann, K.; Marlow, F.; Caro, J. *Adv. Mater.* **1997**, *9*, 567.

(47) Rochon, P.; Batalla, E.; Natansohn, A. *Appl. Phys. Lett.* **1995**, *66*, 136.

(48) Kim, D. Y.; Tripathy, S. K.; Li, L.; Kumar, J. *Appl. Phys. Lett.* **1995**, *66*, 1166. Viswanathan, N. K.; Kim, D. Y.; Bian, S.; Williams, J.; Liu, W.; Li, L.; Samuelson, L.; Kumar, J.; Tripathy, S. K. *J. Mater. Chem.* **1999**, *9*, 1941.

(49) Sekkat, Z.; Wood, J.; Aust, E. F.; Knoll, W.; Volksen, W.; Miller, R. D. *J. Opt. Soc. Am. B* **1996**, *13*, 1713. Sekkat, Z.; Wood, J.; Knoll, W.; Volksen, W.; Miller, R. D.; Knoesen, A. *J. Opt. Soc. Am. B* **1997**, *14*, 829. Sekkat, Z.; Wood, J.; Knoll, W.; Volksen, W.; Lee, V. Y.; Miller, R. D.; Knoesen, A. *Polym. Preprints, Am. Chem. Soc. Div. Polym. Chem* **1997**, *38*, 977.

(50) Sekkat, Z.; Knoesen, A.; Lee, V. Y.; Miller, R. D. *J. Polym. Sci., Part B: Polym. Phys.* **1998**, *36*, 1669. Sekkat, Z.; Prêtre, Ph.; Knoesen, A.; Volksen, W.; Lee, V. Y.; Miller, R. D.; Wood, J.; Knoll, W. *J. Opt. Soc. Am. B* **1998**, *15*, 401.

(51) Kleideiter, G.; Sekkat, Z.; Kreitre, M.; Dieter Lechner, M.; Knoll, W. *J. Mol. Struct.* **2000**, *521*, 167.

(52) Isenbach, C. D. *Bunsen-Ges. Ber. Phys. Chem.* **1980**, *84*, 680.

(53) Williams, M. L.; Landel, R. F.; Ferry, J. D. *J. Am. Chem. Soc.* **1955**, *77*, 3701.

(54) Sekkat, Z. Private communication, Paris-Sud University, 1992.

(55) Sekkat, Z.; Dumont, M. *Synth. Met.* **1993**, *54*, 373. Sekkat, Z.; Knoll, W. *J. Opt. Soc. Am. B* **1995**, *12*, 1855.

(56) Gauglitz, G. In *Photochromism Molecules and Systems*; Bouas-Laurent, H., Dürr, H., Eds.; Elsevier: Amsterdam, 1990; Chapter 2, pp 15−63.